Simple Microwave Technique for Independent Measurement of Sample Size and Dielectric Constant with Results for a Gunn Oscillator System

MYSORE R. LAKSHMINARAYANA, LARRY D. PARTAIN, MEMBER, IEEE, AND W. ALLAN COOK

Abstract—**Standard perturbation theory analysis has been used to develop a new microwave technique for simultaneously and independently measuring the size and dielectric constant of dielectric samples. Gunn flange oscillators have been used to show that simple and low cost systems give measurement accuracies better than 5 percent when applied to nylon, Teflon, and quartz samples. The techniques should be particularly useful with samples of irregular cross section.**

I. Introduction

MICROWAVE measurements enjoy distinct advantages in requiring no mechanical contact with a sample, in response speed to parameter variations, and in operation in continuous or pulsed modes. These and other characteristics have led to a range of microwave measuring systems [1]. A desirable property for such systems would be the ability to determine separately the values for multiple parameters which are changing simultaneously. This paper describes such a technique for the simultaneous measurement of sample size and dielectric constant that is well modeled by theory. Results for simple Gunn oscillator systems are presented to show the close match between actual operation and the model. By comparison, this multiple parameter measuring approach is much simpler and potentially cheaper than previous systems designed to measure only dielectric constant [1], [2] or size [3]. Because dielectric constant is a strong function of moisture content and has some dependence on temperature, these techniques may also be simpler than current microwave methods used for measuring these nonelectrical parameters [3], [4].

II. Frequency Shift Theory

The basic approach is to monitor the resonant frequency shift of a cavity disturbed by the insertion of a rod-shaped sample when the microwave electric field is either parallel or perpendicular to the axis of the sample. If the volume of the sample V_s is small compared to the volume of the air-filled cavity V_c, then standard perturbation theory [1], [5], [6] gives such a frequency shift Δf for nonmagnetic samples as

$$\frac{\Delta f}{f_0} = \frac{\epsilon_0(\epsilon'-1)\int_{V_s} \vec{E}_0\cdot\vec{E}_p\,dV}{\int_{V_c}(\epsilon_0\vec{E}_0\cdot\vec{E}_0-\mu_0\vec{H}_0\cdot\vec{H}_0)\,dV} \tag{1}$$

where ϵ_0 and μ_0 are the permittivity and permeability of free space, respectively, f_0 is the resonant frequency of the unperturbed cavity, and ϵ' is the relative (and real) permittivity of the sample. The $\vec{E}$'s and $\vec{H}$'s are, respectively, the electric and magnetic fields with the subscripts "0" and "p" denoting unperturbed and perturbed values. The subscript V_s and V_c by the integral signs indicate integration over these respective volumes. When f_0 exceeds the perturbed frequency, Δf is taken as positive.

For a rectangular cavity resonating in the TE_{101} mode, a cylindrical sample can be inserted into the center of the cavity through small holes, so that it is parallel to the maximum electric field [1], [7], [8] as shown in Fig. 1(a). Substitution into (1) then gives

$$\frac{\Delta f}{f_0} = 2(\epsilon'-1)\frac{A_s b}{V_c} \tag{2}$$

where $V_s = A_s b$, and A_s and b are, respectively, the cross-sectional areas of the sample and the height of the cavity. For the sample inserted perpendicular to the maximum electric field as shown in Fig. 1(b), the frequency shift is

$$\frac{\Delta f}{f_0} = \frac{2(\epsilon'-1)}{(\epsilon'+1)}\frac{A_s a}{V_c} \tag{3}$$

where a is the width of the cavity since $V_s = A_s a$. This gives two independent equations in ϵ' and A_s for the frequency shift.

Similar results can be obtained with a cylindrical cavity for the sample inserted along the cavity axis as shown in Fig. 2. If the cavity is excited in the TM_{010} mode, the electric field is parallel to the sample [7], [8] and the frequency shift, specified by (1), simplifies to

Manuscript received May 22, 1978; revised August 11, 1978. This work was part of a dissertation submitted in June 1978, by M. R. Lakshminarayana to the Faculty of the University of Delaware, Newark, in partial fulfillment of the requirements for the Ph.D. degree.

M. R. Lakshminarayana and L. D. Partain are with the Department of Electrical Engineering, University of Delaware, Newark, DE 19711.

W. A. Cook is with the Engineering Physics Laboratory, E.I. DuPont Company, Wilmington, DE 19898.

0018-9480/79/0700-0661$00.75 ©1979 IEEE

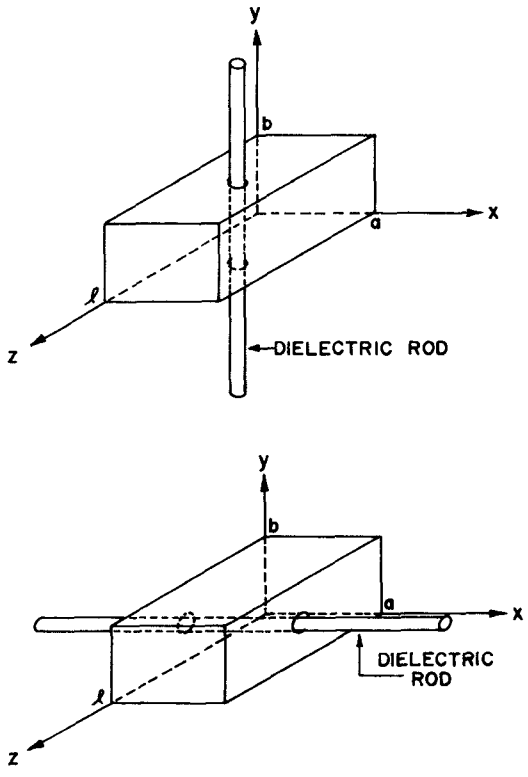

Fig. 1. TE_{101}-mode rectangular cavity.

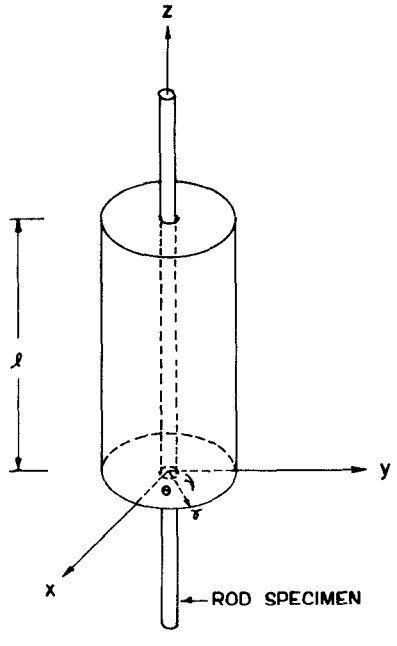

Fig. 2. Cylindrical cavity with a dielectric rod along its axis.

$$\frac{\Delta f}{f_0} = \frac{(\epsilon' - 1)}{2J_1^2(\chi)} \frac{A_s l}{V_c} \tag{4}$$

where l is the length of the cavity, and $J_1(\chi) = 0.5191$ is the first-order Bessel function of the first kind, with $\chi = 2.405$ the first zero of the zeroth-order Bessel function of the first kind.

If this cavity is excited in the TE_{112} mode, the electric field becomes perpendicular to the sample, and the frequency shift is given by

$$\frac{\Delta f}{f_0} = \frac{\epsilon' - 1}{\epsilon' + 1} \frac{1}{2(1 - 1/\chi^{*2})J_1^2(\chi^*)} \frac{A_s l}{V_c} \tag{5}$$

where $\chi^* = 1.841$ is the first zero of the derivative of the first-order Bessel function of the first kind that gives $J_1(\chi^*) = 0.5819$. Once again two independent equations in ϵ' and A_s are obtained. Identification of which of the various cylindrical modes is being excited can be accomplished by monitoring the resonant frequency [7], [9].

Separation of the variables ϵ' and A_s from measured Δf values requires two independent equations. For the rectangular cavity case, solution of (2) and (3) gives

$$\epsilon' = \frac{a}{b} \frac{[V_c(\Delta f/f_0)]_{\|}^r}{[V_c(\Delta f/f_0)]_{\perp}^r} - 1 \tag{6}$$

where the superscripts r refer to the rectangular cavity, and the subscripts $\|$ and $\perp$, respectively, identify which measured $\Delta f/f_0$ values were obtained for the electric field parallel and perpendicular to the sample. If the same size cavities or a single cavity is used for both the parallel and perpendicular measurements, the cavity volumes V_c, of course, cancel out. Substitution of ϵ' back into either (2) or (3) then gives the sample cross-sectional area A_s.

Similarly, for the cylindrical cavity cases

$$\epsilon' = \frac{[J_1^2(\chi) V_c(\Delta f/f_0)]_{TM}^c}{[J_1^2(\chi^*) V_c(1 - 1/\chi^{*2})(\Delta f/f_0)]_{TE}^c} - 1 \tag{7}$$

where the subscripts specify the values applicable for the TM_{010} and TE_{112} modes, and where the superscript c identify the cylindrical cavity. Again, if the same cavity is used for both modes, the cavity volumes V_c cancel. Substitution of this ϵ' value back into either (4) or (5) gives the sample size A_s. Other combinations of independent equations (such as (2) and (5) or (3) and (4), or different expressions for other modes) that have the electric field parallel or perpendicular to the sample can also be used to separate these variables.

III. Gunn Oscillator Systems

The configurations shown in Figs. 1 and 2 allow precise theoretical analysis; but in their ideal forms, they provide no means for coupling microwave energy into and out of the cavities. A simple means for driving such cavities without departing too far from ideal behavior is obtained by attaching Gunn flanges to the sides of properly designed cavities.

A rectangular cavity was designed to operate at around 9 GHz in the TE_{101} mode [7]. This had a width of 0.9 in, a height of 0.4 in, and a length of 0.9 in. At the center of opposing broad and narrow walls, $\frac{1}{8}$-in holes were drilled to allow sample insertion like that shown in Fig. 1(a) and (b). A Gunn flange was used to replace one of the end walls (lying in the $X-Y$ plane as shown in Fig. 1). The

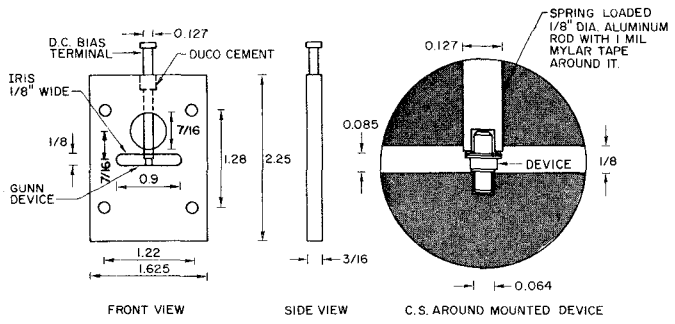

Fig. 3. Flange mounting for Gunn device (all dimensions are in inches).

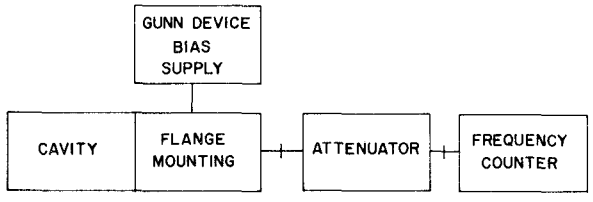

Fig. 4. Microwave transducer setup.

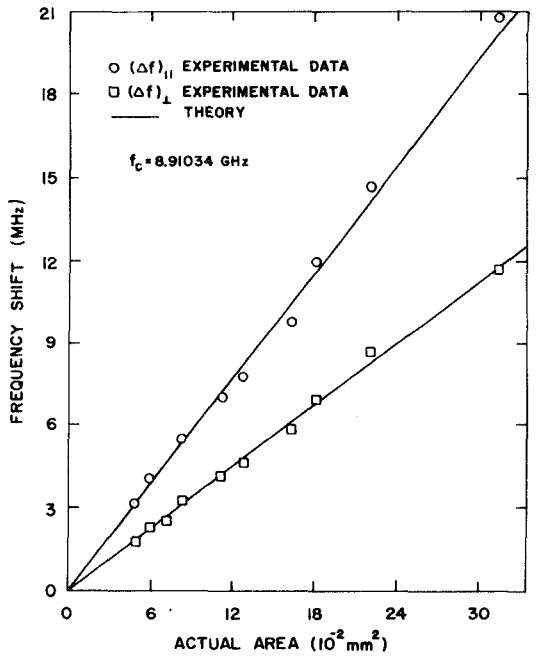

Fig. 5. Plot of frequency shift as a function of actual area for nylon monofilaments in a TE_{101}-mode rectangular cavity.

characteristics of such flanges have been described elsewhere in some detail [10], [11]. The dimensions for this X-band flange are detailed in Fig. 3. A Microwave Associates Gunn Device MA49158 with a 9-GHz center frequency occupied the flange. The flange was oriented so that its bias terminal (see Fig. 3) was parallel to the X direction (Fig. 1) and its iris slot was centered at the cavity end. (More detailed sketches of such an oscillator were shown in an earlier paper [12].) This oscillator was attached to an EIP Model 350D microwave frequency counter through an attenuator and to a dc power supply (0–12 V, 1.0 A) as shown schematically in Fig. 4. With such a cavity-controlled oscillator, the resonant frequency shifts were read directly from the counter. Because the cavities were relatively high Q, the capacitive reactance of the Gunn devices pulled the resonant frequencies by less than two percent from their theoretical values.

A single cylindrical cavity [7] was designed to oscillate at 8.8 GHz in the TM_{010} mode, and at 10.3 GHz in the TE_{112} mode. It had a radius of 0.5 in and length of 1.5 in; $\frac{1}{8}$-in holes as shown in Fig. 2 were made at the center of the cavity ends to allow sample insertion. Little radiation occurred through these or the rectangular cavity holes since interruption of current flow lines was minimal. Incorporation of the Gunn flange onto the cylindrical cavity involved cutting a rectangular iris 0.405 in by 0.980 in halfway along the length l of the cavity, so that the longer iris dimension was perpendicular to the cavity axis (for more details see the sketch shown in the earlier paper [12]). This was connected to the power supply and frequency counter as indicated by Fig. 4.

Switching between the modes was obtained by inserting and withdrawing lossy material (graphite pencil lead) into and out of the cavity at various angles. For small angles to the cylindrical axis, TE_{112} oscillation was obtained. For large angles, TM_{010} oscillation was produced.

IV. Experimental Results

A comparison between the theoretically predicted and experimentally observed frequency shifts with the rectangular oscillator is shown in Fig. 5, as a function of the actual cross-sectional area of the samples obtained by measuring the diameters with a precision micrometer. These data are for rod-shaped nylon samples inserted parallel and perpendicular to the microwave electric field. The observed frequency shift data are in excellent agreement with the solid lines representing the theoretical values specified by (2) and (3).

The ability of these systems to separate sample size and dielectric constant is demonstrated in Figs. 6 and 7. In Fig. 6, the measured dielectric constant for nylon material (calculated from (6)) is presented as a function of the actual sample diameter measured with a precision micrometer. This required that each sample be inserted through the $\frac{1}{8}$-in holes both parallel and perpendicular to the electric field. Typical accuracies of from 2 to 5 percent in determining size and dielectric were found for the rectangular cavity, and from 1 to 3 percent with the cylindrical cavity with nylon, quartz, and Teflon samples.

Good frequency-shift detection sensitivity ($\Delta f > 1$ MHz) is obtained when the ratio of the sample to cavity volume times the relative dielectric constant ($\epsilon' V_s / V_c$) is greater than $2(10^{-4})$ as shown in Fig. 8. This shows that the relative frequency shifts ($\Delta f / f_0$) are of the same order of magnitude for all the systems studied as described by the theoretical expression from Section II. To satisfy the small disturbance assumption, these values should probably remain below 1 percent (i.e., 10^{-2}). Proper choice of cavity frequency (and thus its size) should assure operation in this range for arbitrary sample size. Accurate parameter measurements were obtained for stranded as well as rod-

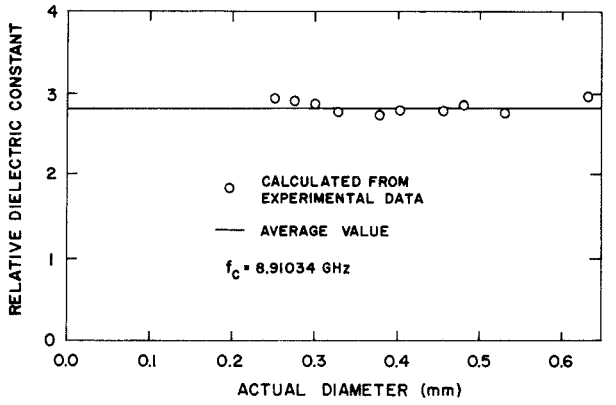

Fig. 6. Calculated relative dielectric constant versus actual diameter for nylon monofilaments in TE_{101}-mode rectangular cavity.

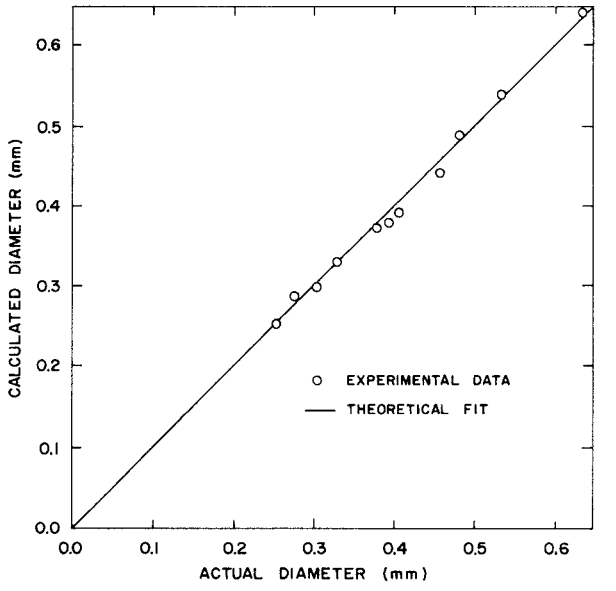

Fig. 7. Calculated diameter versus actual diameter for nylon monofilaments in TE_{101}-mode rectangular cavity.

shaped samples indicating that other than the theoretically ideal cylindrical shape can be measured.

When an IMPATT diode was substituted for the Gunn device in the X-band flange and properly biased, similar results were obtained. Passive cavity measurements of the frequency shifts also gave comparable but lower accuracy results (± 10 percent). For the passive measurements, the Gunn flange was replaced with a small iris; and the cavity was connected to a microwave sweeper. The resonant frequency shift was obtained by observing the frequency (or frequencies for the cylindrical cavity) where minimum microwave energy was reflected from the cavity. Resonant frequency determination in this manner was less accurate than just reading the frequency of a microwave counter as required with the active cavity systems. However, the passive swept-frequency technique did have the advantage of enabling both the TM- and TE-mode resonant frequencies to be measured from a single sweep instead of the switching (or two cavities) required with the cylindrical Gunn oscillator.

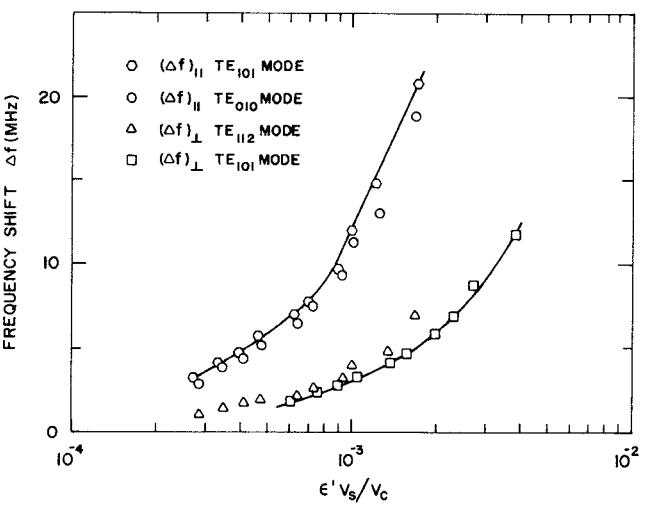

Fig. 8. Frequency shift versus product, dielectric constant times sample volume normalized to the cavity volume for nylon monofilaments in rectangular and cylindrical cavities.

V. Conclusions

Direct application of standard cavity-perturbation theory has led to a straightforward method of parameter separation for sample dielectric constant and sample size. This technique should be particularly useful with samples of irregular cross section. X-band Gunn-flange driven cavities have shown that a close approximation to the theoretical model is obtained with simple and potentially low-cost systems. Actual system costs would be determined primarily by what instrumentation is used for measuring frequency changes, and by the number of cavities measured by this instrumentation since the Gunn oscillators themselves are relatively low cost. The measurement accuracy attained in this study was typically 5 percent or better. Good parameter-separation performance was also achieved with IMPATT driven and passive cavities. Parameters related to dielectric constant such as moisture and temperature should also be measureable by these techniques.

References

[1] M. Sucher and J. Fox, Eds., *Handbook of Microwave Measurements*. New York: Polytechnic, 1963.
[2] P. Nagenthiram and A. L. Cullen, "A microwave barrel resonator for permittivity measurements on dielectric rods," *Proc. IEEE*, pp. 1613–1614, Nov. 1974.
[3] S. S. Stuchly and M. A. K. Hamid, "State of the art for measuring non-electrical quantities," *Int. J. Electron.*, vol. 33, pp. 617–633, 1972.
[4] M. A. K. Hamid and N. J. Mostowy, "Open circuit step cavity resonator for continuous monitoring of sheet moisture content," *Int. J. Electron.*, vol. 37, pp. 511–520, 1974.
[5] H. B. G. Casimir, "On the theory of electromagnetic waves in resonant cavities," Philips Research Rep., vol. 6, pp. 162–182, 1951.
[6] R. A. Waldron, *The Theory of Waveguides and Cavities*. New York: Gordon and Breach Science, 1969.
[7] A. J. Baden Fuller, *Microwaves*. 1st ed. New York: Pergamon, 1969.
[8] N. Marcuvitz, Ed., *Waveguide Handbook*. M.I.T. Radiation Laboratory Series, vol. 10, New York: McGraw-Hill, 1951.
[9] H. R. L. Lamont, *Waveguides*. 3rd Ed. New York: Wiley, 1950.
[10] J. Bybokas and B. Farrell, "The Gunn flange—A building block

for low-cost microwave oscillators," *Electronics*, vol. 44, pp. 47–50, Mar. 1, 1971.
[11] T. P. Lee and R. D. Standley, "Frequency modulation of a millimeter—Wave IMPATT diode oscillator and related harmonic generation effects," *Bell System Tech. J.*, vol. 48, pp. 143–161, Jan. 1969.
[12] L. D. Partain, W. A. Cook, H. Huang, and L. C. Goodrich, "Absolute load detection with microwave Gunn oscillators," *IEEE Trans. Microwave Theory Tech.*, vol. MTT-24, pp. 656–660, Oct. 1976.

Conversion Losses in Schottky-Barrier Diode Mixers in the Submillimeter Region

WILLIAM M. KELLY AND GERARD T. WRIXON, MEMBER, IEEE

Abstract—**Conversion losses, both intrinsic and parasitic, are calculated for Schottky diode mixers in the submillimeter region, and optimum mixer performance is shown to depend strongly upon operating frequency and upon diode diameter. The implications for high-frequency diode fabrication are discussed, and a comparison is made of the expected performance of GaAs, Si, and InSb Schottky diodes at frequencies up to 5 THz.**

I. Introduction

RECENT interest in the development of sensitive low-noise heterodyne spectrometers in the submillimeter region of the spectrum has created a need for nonlinear mixing elements which will perform efficiently at wavelengths shorter than a millimeter. The role of mixing element at millimeter wavelengths is normally filled by Schottky-barrier diodes made on epitaxial GaAs, and in this paper we wish to consider quantitatively, how these diodes may be expected to perform at frequencies over 300 GHz.

The conversion loss L of a mixer is the ratio of the available power from the RF source to the power absorbed in the IF load. A large fraction of this conversion loss occurs in the diode, arising from two separate processes, the intrinsic conversion loss L_0 and the parasitic conversion loss L_p, with $L = L' L_0 L_p$. L_0 is the result of losses arising from the conversion process within the nonlinear resistance of the diode and for a broadband mixer has a theoretical minimum of 3 dB. L_p is the loss associated with the parasitic elements of the diode, namely, the junction capacitance C_0 and the series resistance R_s. Finally, L' is the total loss from other sources in the mixer, e.g., ohmic losses in the RF and IF circuits, mismatch losses, etc.

Manuscript received October 7, 1978; revised January 22, 1979. This paper was sponsored by the European Millimeter Diode Laboratory, University College, Cork, Ireland.

The authors are with the Department of Electrical Engineering, University College, Cork, Ireland.

The parasitic and intrinsic conversion losses L_p and L_0 will be discussed in detail below. The figure of merit which is normally used in evaluating the high-frequency performance potential of a Schottky-barrier diode is the cutoff frequency $f_c = 1/2\pi R_s C_0$. In view of the fact that R_s is frequency dependent [1] and f_c, as thus defined, can actually be multivalued, cutoff frequency is not a useful performance criterion at short wavelengths. Instead we examine in detail the behavior of L_p and L_0, which can be calculated if R_s and C_0 are known. The determination of R_s as a function of operating frequency is included in Section II below, followed by the calculation of parasitic loss L_p in Section III. In Section IV, intrinsic conversion loss L_0 is examined. Finally, in Section V, total conversion losses are calculated as a function of diode size for various frequencies. The results indicate that for a given operating frequency there is an optimum diode size which minimizes losses, irrespective of f_c. This conversion-loss minimum increases in value with frequency. Based upon our results we predict the performance which may be expected of state-of-the-art diodes in the submillimeter region, and discuss their implications for future diode fabrication.

II. Series Resistance

Fig. 1(a) shows the cross-sectional details of a typical n/n^+ Schottky-barrier diode as used at millimeter wavelengths. The chip is fabricated by growing a thin ($\approx$0.2-μm) epitaxial layer of carrier concentration $\sim 2\times10^{17}$ cm^{-3} on to a low resistivity n^+ substrate ($n^+ > 2\times10^{18}$ cm^{-3}) typically, 100 μm thick. The bottom of the substrate has an alloyed ohmic contact [2] while the front surface is covered with an SiO_2 passivation layer. Circular holes are opened in the SiO_2 photolithographically, and the Schottky barrier is formed by depositing Pt followed by Au through the holes onto the GaAs epilayer.

A simple equivalent circuit for this diode is shown in Fig. 1(b) consisting of the nonlinear barrier resistance R_0

0018-9480/79/0700-0665$00.75 ©1979 IEEE